

Individual NW Chemical Composition Depth Profiling and Surface Oxidation Analyzed by Auger Electron Spectroscopy

U. Givan*, J. Hammond**, D. Paul** and F. Patolsky*

*Tel-Aviv University, Tel-Aviv, Israel, urigivan@post.tau.ac.il.

** Physical Electronics Inc., 18725 Lake Drive East, Chanhassen, MN, USA, 55317, jhammond@phi.com

** Physical Electronics Inc., 18725 Lake Drive East, Chanhassen, MN, USA, 55317, dpaul@phi.com

*Tel-Aviv University, Tel-Aviv, Israel, fernando@post.tau.ac.il.

ABSTRACT

Nanowires (NWs), as well as other nanoscale structures, are in the heart of extensive study over the last few decades for both scientific and application interests. NWs physical properties are profoundly dependent on their surface chemical composition and size, prompting the need for the challenging characterization of an **individual** NW. Recent instrumentation advances in Field Emission Scanning Auger combined with sputter ion depth profiling allow the analysis of the lateral and depth elemental distributions of individual NWs.

In this study, a series of CVD-VLS grown, SiGeNWs and phosphorus doped SiNWs were characterized by Scanning Auger with a sub 10 nm primary electron beam. The lateral concentrations of oxide, silicon, germanium and phosphorus were obtained as a function of the NW's diameter showing the nature and depth of the surface oxidation and the Si/Ge ratio radial homogeneity in SiGeNWs. In addition, initial results of depth dependent phosphorus doping concentrations were obtained. **Keywords:** "scanning Auger microscopy" "doping" "depth profiling" "silicon nanowire" "silicon germanium nanowire"

1 INTRODUCTION

The rapidly growing interest in novel nanostructure based applications requires the integration of complicated heterostructures and superlattices leading to new fabrication and analytical characterization challenges. Specifically, the study of the interplay between fabrication processes and the resulting nanostructure size dependent properties requires the use of analytical tools with nanometer scale probing capabilities. For example, doped silicon nanowires (SiNWs) based FET devices are being evaluated as promising candidates for replacing traditional MOSFETs, prompting the requirement to understanding their unique electronic properties. Nevertheless, only recently has an appropriate analytical tool lead to the correlation of the inhomogeneous radial dopant concentration to the doped SiNWs high resistivity [1-2].

Auger electron spectroscopy (AES) is one of the most widely used analytical techniques for high spatial resolution analysis of the chemical composition of solid surfaces. Its surface sensitivity of 0.5 nm-2 nm combined with sub-micron SEM and Auger spatial resolution and the ability to detect and quantify all elements above helium has led to the scanning Auger microscope (SAM) becoming a standard analytical tool in both research laboratories and production support laboratories in the microelectronics industry. The development of new nm scale electron probe beams combined with ion beam sputter depth profiling has made the new generation of Scanning Auger Nanoprobe a promising analytical tool for emerging research in nanotechnology.

In this study the elemental and chemical depth compositions of individual NWs were analyzed by a nanoprobe SAM. Previous direct analytical measurements of the depth distributions on NWs have only been reported with the infrequently used atom probe tomography (APT) [1]. Mostly indirect measurement techniques have also been extensively employed in recent years which showed that the dopant profiles were inhomogeneous [1, 3-7]. The dopant profiles in this study are in agreement with previous studies and demonstrate that the nanoprobe SAM is a simple alternative for the complicated APT technique and can be used as a direct measurement technique compared to previous indirect measurement techniques. The chemical composition depth profiling of SiGeNWs is also reported. Previous research has studied the miscibility of Si and Ge in SiGeNWs employing Raman spectroscopy to detect Ge segregation [8-9]. The present findings show no signs of inhomogeneity in the Si/Ge ratio and are in agreement with TEM-EDS measurements.

2 EXPERIMENTAL

2.1 Si_(1-x)Ge_xNWs and SiNWs Growth

The growth procedures for phosphorus doped SiNWs and Si_(1-x)Ge_x NWs have previously been described in detail [10]. In summary, all NWs produced for this study were grown by the VLS technique in a hot-wall CVD set-up, with 20 nm gold nanoparticles (AuNPs) as the catalyst,

high-purity silane (SiH₄) and germane (10% GeH₄ in H₂ carrier) as precursor and dopant gases, and hydrogen as the carrier gas. Phosphine (1000 ppm in H₂ carrier) served as the N-doping gas. Silicon substrates were dipped in a solution of poly-L-lysine, washed with deionized distilled water (DDW), and dried in a stream of dry nitrogen. After drying, the substrates were dipped in a diluted solution of AuNPs, washed and dried as described above. Finally, organic traces were removed by oxygen plasma. Substrates were then placed at the center of a horizontal quartz tube in a hot-wall furnace, which was then evacuated and purged in a stream of argon and hydrogen. Flow rates were determined with the use of mass-flow controllers (MFC), and the pressure in the growth chamber was computer-controlled via a throttle valve that limited the flow to the vacuum pump. In order to suppress radial growth, the following growth parameters were chosen for Si(1-x)Ge_x NWs: growth temperature - 3500C; inlet-gas ratio (GeH₄/(GeH₄+SiH₄)) - 0.02. The inlet-gas flows were: 10%GeH₄ -1 sccm (standard centimeter cube per minute at STP), SiH₄ - 5sccm, H₂ -100 sccm. The growth parameters of the 1/2000 phosphorus doped SiNWs were: growth temperature - 5000C. The inlet-gas flows were: SiH₄ - 4 sccm, H₂ -20 sccm. Phosphorus doping was carried out by adding a PH₃ flow of 2 sccm during growth. Growth times varied from 20 to 5 minutes, resulting in 35 to 30 μm long NWs. The growth process was ended by purging the sample with argon and hydrogen while it was cooling.

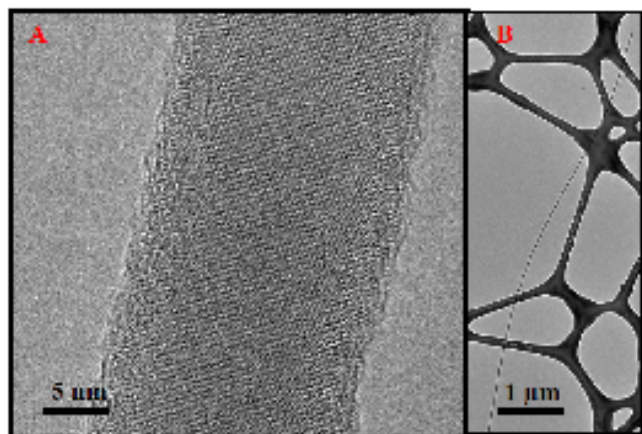


Figure 1: TEM images of slightly tapered typical 1/2000 phosphorus doped SiNW (B), with 20nm diameter (A).

2.2 Sample Preparation

NWs were removed from the growth substrate by sonication in isopropanol. The NWs containing solution was dispersed onto GaAs substrates for SAM measurements or onto lacey carbon-coated copper grids for TEM analysis. Prior to NWs deposition, E-beam lithography and thermal evaporation were used to pattern the GaAs substrates with 30 μm Au crosses grid. After NWs deposition the pattern was used for samples mapping via dark field optical microscopy.

2.3 Auger measurements

The Auger data was acquired with a Physical Electronics PHI 700Xi Scanning Auger equipped with a 25 kV Schottky field emission electron gun and a coaxial Cylindrical Mirror Analyzer (CMA). The base pressure of the PHI 700Xi is $< 6.7 \times 10^{-8}$ Pa ($< 5 \times 10^{-10}$ Torr). All secondary electron images, Auger spectra and Auger depth profiles were acquired with a 20 kV electron beam with an incident current on the sample of 5 nA with a probe diameter of 9.5 nm. The Auger data was acquired at 0.5% CMA energy resolution for elemental identification and for calculations of surface atomic concentration. All atomic concentration calculations used $dN(E)/dE$ peak to peak height measurements. High energy resolution spectra of Ge LMM spectra and Si KLL spectra on a SiGeNW were acquired at 0.1% CMA energy resolution and displayed in the N(E) mode after a polynomial background subtraction.

Depth profiling of the SiGeNWs and the phosphorous doped SiNWs was performed using an alternating Auger data acquisition with 500 eV Argon ion sputtering. Each sputtering cycle was for 20 seconds resulting in a sputter rate of 1 nm per cycle, as calibrated on a standard SiO₂ thin film. A computer controlled image registration of the beam position was used to maintain precise electron beam alignment during the high sensitivity depth profiling. The presence of the low concentration P dopant was verified by the exact phosphorous LMM N(E) peak position and the atomic concentration values as a function of depth were calculated using the $dN(E)/dE$ peak to peak heights of the P LMM and Si KLL spectra and PHI supplied sensitivity factors.

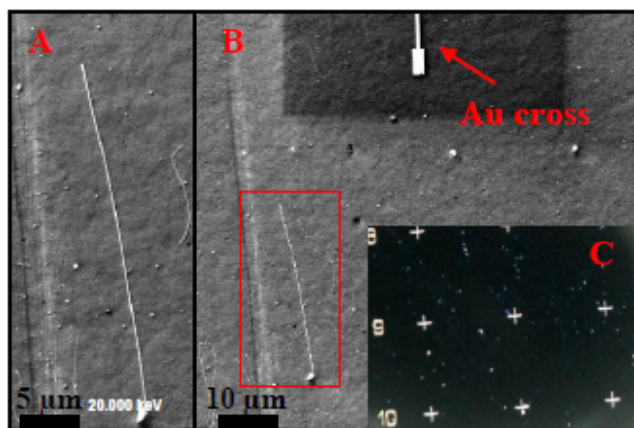


Figure 2: The SEM capacity of the PHI700 enables detection and focusing the e-gun on individual NW without undesired carbon coating. "in-situ" SEM image of individual SiNW: (A) - a 30 μm SiNW on GaAs substrate (the enclosed area in B). (B) - lower magnification SEM image showing the SiNW and the Au cross ending, the inset (c)- Dark field optical image of patterned GaAs substrate after NWs deposition .

3 RESULTS AND DISCUSSION

3.1 Si_(1-x)Ge_xNWs

The Si_(1-x)Ge_xNW morphology, crystalline structure and chemical composition were studied with SEM, TEM and EDS prior to the scanning Auger in depth chemical analysis. The NWs were found to be: 20-30 nm diameter, up to 30 μm length, single crystalline structure with a smooth, thin amorphous Si shell layer. EDS results have shown the NWs to be 45% Si and 55% Ge (Si_{0.45}Ge_{0.55}NWs). Auger scans of a 30 nm thick Si_{0.45}Ge_{0.55}NW revealed the following elements: Si, Ge, Ga, As, O and C. Comparing the scans taken on the Si_{0.45}Ge_{0.55}NW to scans taken on the GaAs substrate has shown similar carbon percentages. The carbon percentages of both the substrate and the Si_{0.45}Ge_{0.55}NW decreased after each round of Ar⁺ etching, leading us to conclude that the carbon contamination covered the entire sample and was eliminated after a few nm of etching. In contrast, the oxygen percentages on the Si_{0.45}Ge_{0.55}NW were found to be higher than those found on the substrate and substantially decreased only after 3-5 nm of etching. This observation was reinforced by the broadening of the Si peak attributed to SiO which disappeared after the same etching depth. From both observations we conclude that the measured oxygen originated in ~5 nm width of the amorphous shell.

Figure 3A shows the differential (dN(E)/dE) scan results over the entire energy range taken after 1 nm etching with observable peaks from all of the above mentioned elements. The Si peak broadening is shown in figure 3B. The same broadening was observed in both the as received and after 4 nm etching Auger scans. After additional etching the broadening was no longer observed. The Si/Ge atomic concentrations as a function of sputter depth, presented in figure 3C, were obtained by further etching and Auger analyses in 1 nm intervals. The Si/Ge ratios are similar to the TEM-EDS results throughout almost the entire NW's width. A 7% increase in the Si percentage was observed after ca. 15 nm of etching which seems to exceed the measurement noise level (ca. 2%).

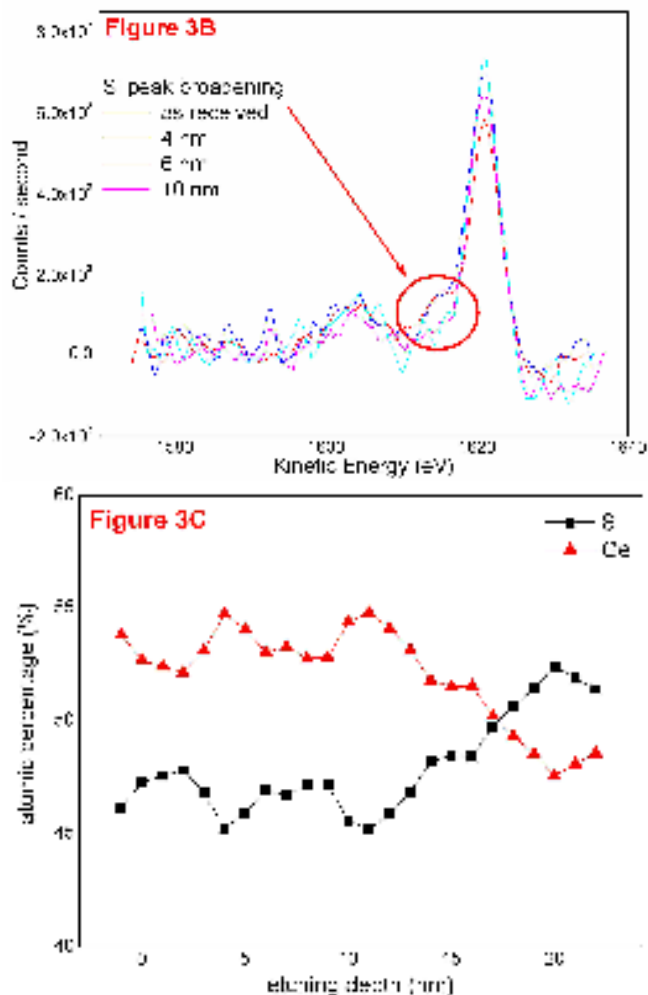
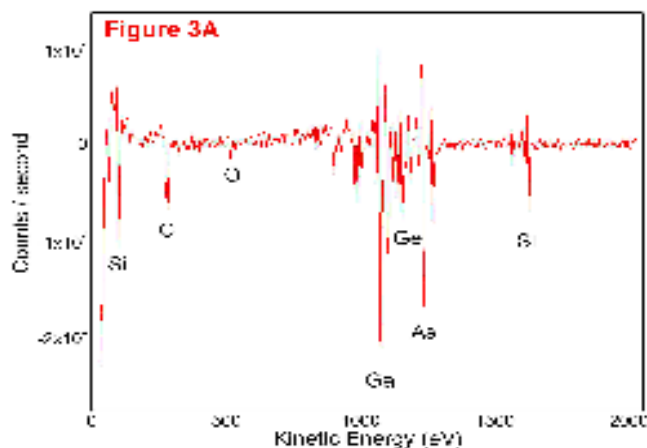


Figure 3: Auger measurements of Si_{0.45}Ge_{0.55}NW. (A)- Differential mode Auger scan (prior to etching). (B)- The Si Auger peak at various depths. (C)- compositional depth profiling.

3.2 Phosphorus doped SiNWs

Figure 4A shows the differential mode Auger scan results of the entire energy range taken from a 1/2000 phosphorus doped SiNW before etching. Ga, As, Si, O, C and P elemental peaks are readily observable. The calculated atomic percentage values of Si and Ge were similar to those measured of SiGeNWs. Comparable reduction of carbon by the Ar⁺ sputtering was observed for both the SiNW and the GaAs wafer suggesting that the surface contamination is easily eliminated. The oxygen concentration was substantially reduced after 5-6 nm of etching in a similar manner observed with the SiGeNWs. Surprisingly high phosphorus concentrations close to 1% were observed at the SiNW's surface. The phosphorus concentration was dramatically reduced with further etching. The phosphorus detectability limit is determined by the signal to noise limit of the observable Auger

phosphorous LMM peak and was found to be $\sim 1/1250$. Nevertheless, we believe that lower concentrations may be detected with further improvements of the measurement conditions.

The radial distribution of phosphorus dopant concentration is presented in figure 4B. The phosphorous atomic concentration depth profile shows a 1/120 phosphorus to silicon ratio on the NW's surface which decreases to about 1/350 after 8 nm etching. The high dopant ratios (as compared to the 1/2000 phosphorus to silicon inlet gases ratio) might be the outcome of the specific NW's growth conditions- in this case the NW was grown at 500°C and was slightly tapered.

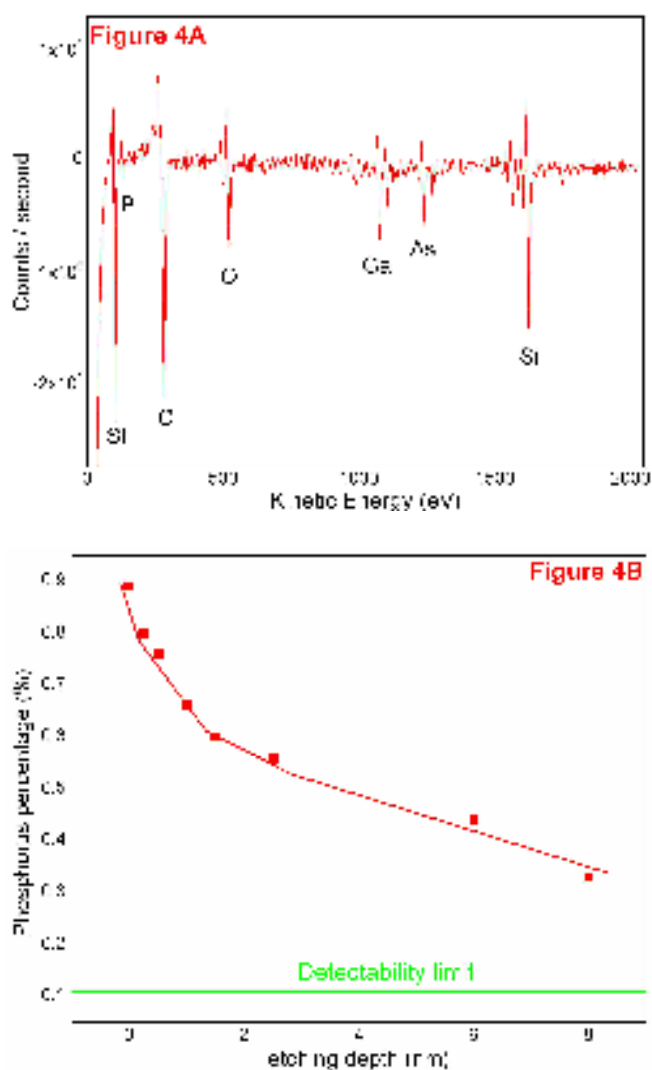


Figure 4. Scanning Auger chemical analysis of a phosphorus doped SiNW (A)- full energy range scan in differential mode. (B)- Depth profiling reveals the non-homogenous radial phosphorus doping distribution.

4 SUMMARY

In conclusion, successful analysis of the lateral and depth elemental distributions of individual NWs was achieved employing a nanoprobe field emission scanning Auger combined with low voltage sputter ion depth profiling.

The surface of $\text{Si}_{0.45}\text{Ge}_{0.55}\text{NWs}$ was studied and found to be composed of 4-6nm SiO layer with no evidence for GeO . The $\text{Si}_{0.45}\text{Ge}_{0.55}\text{NWs}$ in depth chemical analysis was obtained by further etching and the atomic fractions were in agreement with previously obtained TEM-EDS results. The compositional depth profiling revealed the Si/Ge ratio to be constant throughout the first 15nm with some 5 nm cyclic diversity of 2%. An increase of 7% in the Si atomic percentage was found closer to the $\text{Si}_{0.45}\text{Ge}_{0.55}\text{NW}$ core. Further study is needed to verify both findings (the cyclic behavior and the Si rich core).

The nanoprobe scanning Auger was found to be relevant for depth compositional analysis of individual phosphorus doped SiNWs. The dopant concentration distribution profile was found to be rapidly decreasing with depth, starting with over 15 fold higher concentration values at the NW's surface than the expected values from the inlet gas ratio (1/2000). The inhomogeneous distribution is in agreement with previous direct measurements (carried out with APT), indirect measurements and theoretical predictions. The detectability limit was found to be $\sim 1/1250$. We believe this value could be substantially decreased by further improvement of technical measurement conditions.

REFERENCES

- [1] D. E. Perea, E et al, *Nature Nanotechnology*, 4, 315, 2009.
- [2] V. Schmidt, et al, *Adv. Mater.*, 21, 2681, 2009.
- [3] J. E. Allen, et al, *Adv. Mater.*, 21, 1, 2009.
- [4] E. C. Garnett, et al, *Nature Nanotechnology*, 4, 311, 2009.
- [5] E. Koren, et al, *Nano Lett.*, 10, 1163, 2010.
- [6] P. Xie, Y. et al, *Proc. Natl. Acad. Sci. USA* 106, 15254, 2009.
- [7] E. Koren, et al, *Appl. Phys. Lett.* 95, 92105, 2009.
- [8] Q. Lu, et al, *J. Phys. Chem. C*, 112, 3209, 2008.
- [9] C. Nishimura, et al, *Appl. Phys. Lett.* 93, 203101, 2008.
- [10] U. Givan, F. Patolsky, *Nano Lett.*, 9, 1775, 2009.